On the Simulation of Surface-Plant-Air Interactions Inside Urban Environments

Michael Bruse and Heribert Fleer
Researchgroup Climatology, Institute for Geography, University of Bochum, Germany

Abstract In recent years high-resolution numerical simulation of surface-plant-air interactions as an important part of global circulation models (GCM) or as a tool to assist in planing decisions has experienced increased consideration. In contrast to mostly indolent large scale phenomena described in GCMs, the lower part of the atmosphere where we live is very sensitive to small scale processes which can develop an individual local climate, different to the expected average conditions. Especially in urban areas the great variety of different surfaces and sheltering obstacles produces a pattern of distinct microclimate systems. To simulate these local effects, microscale surface-plant-air interaction schemes with a special extension to typical artificial urban boundaries are needed. The paper focuses on the microscale numerical simulation of surface-plant-air interactions inside urban structures, especially the feedback between artificial surfaces like buildings and vegetation inside street canyons, backyards or greens. Three-dimensional non-hydrostatic model ENVI-met is presented and used to solve the basic equations forward in time and can simulate "hard" wind field modifications (solid boundaries) like walls as well as "soft" modifications (porous shelters) like vegetation. A case study presents some effects of vegetation on flow, temperature and turbulence near to and between buildings. It is shown that even small modifications can cause big variations in the structure of flow, and temperature fields.

1. INTRODUCTION

Climate modification in urban environments has been the scope of several numerical models in the past.
Starting somewhere in the early seventies with quite general macroscale approaches analyzing the interactions between urban and rural areas (Hirt & Cook 1972, Gutman and Torrance, 1975) urban climate models improved parallel to available computer resources. More powerful computers allowed to increase the number of considered processes as well as the resolution of the models. In the beginning of the eighties a new generation of models began to focus on small scale processes inside urban structures themselves.
Due to restricted computer resources, models still had to concentrate on one special aspect of urban climate, for example energy fluxes at surfaces (URBAN3, Terjung and O'Rourke, 1980) or the modification of air flow near to obstacles (MISKAM, Eichhorn 1989).
As a matter of fact, microscale processes are linked to each other and cannot be generalized without loosing more or less of their dynamic characteristics. Especially the effect of vegetation on turbulent flow or heat and vapor fluxes is mostly neglected in microscale urban models although a wide range of comprehensive numerical models for plant-air interactions are available (for example Wang and Takle, 1995; Liu et al., 1996; Watanabe, 1994)

This paper presents the model ENVI-met which is able to simulate microscale interactions between urban surfaces, vegetation and the atmosphere. ENVI-met allows to analyze the effects of small scale changes in urban design (e.g. trees, backyard greening, new building constellations) on microclimate under different mescoscale conditions.

2 THE ATMOSPHERIC MODEL

2.1 Mean Air Flow

The basic concept to describe three-dimensional turbulent flow is given by the non-hydrostatic incompressible Navier-Stokes equations (1-a) - (1-c):

$$\frac{\partial u}{\partial t} + u_i \frac{\partial u}{\partial x_i} = -\frac{\partial p'}{\partial x} + K_m\left(\frac{\partial^2 u}{\partial x_i^{\,2}}\right) + f(v - v_g) - S_u \qquad (1\text{-a})$$

$$\frac{\partial v}{\partial t} + u_i \frac{\partial v}{\partial x_i} = -\frac{\partial p'}{\partial y} + K_m\left(\frac{\partial^2 v}{\partial x_i^{\,2}}\right) - f(u - u_g) - S_v \qquad (1\text{-b})$$

$$\frac{\partial w}{\partial t} + u_i \frac{\partial w}{\partial x_i} = -\frac{\partial p'}{\partial z} + K_m\left(\frac{\partial^2 w}{\partial x_i^{\,2}}\right) + g\frac{\theta(z)}{\theta_{ref}(z)} - S_w \qquad (1\text{-c})$$

$$\frac{\partial u}{\partial x} + \frac{\partial v}{\partial y} + \frac{\partial w}{\partial z} = 0 \qquad (1\text{-d})$$

where f ($=10^4$ sec^{-1}) is the Coriolis parameter, p' is the local pressure perturbation, θ is the potential temperature at level z and θ_{ref} is a reference temperature at the same level.
Air density ρ was removed from the original compressible equations using the *Boussinesq-Approximation* which leads to one additional term in the w-equation to include thermal forced vertical motion and one continuity equation (1-d) to be satisfied for each time step in order to keep the model mass conserving. Note that all three-dimensional advection and diffusion terms are written in Einstein summation (u_i=u,v,w i=1,2,3) to save place.
S_u, S_v and S_w describe the loss of wind speed due to drag forces at vegetation elements. Following Liu [1996] and Yamada [1982] this effect can be parameterized as

$$S_{u(i)} = \overline{\frac{\partial p'}{\partial x_i}} = c_{d,f} LAD(z) \cdot W \cdot u_i \qquad (2)$$

$W=(u^2+v^2+w^2)^{0.5}$ is the mean wind speed at height z, LAD(z) is the leaf area density in $m^2m^{-3}$of the plant in this height. The mechanical drag coefficient at plant elements $c_{d,f}$ is is set to 0.2.

2.2 Temperature and Humidity

The distribution of temperature θ and specific humidity q inside the atmosphere is given by the combined advection-diffusion equation with internal source/sinks :

$$\frac{\partial \theta}{\partial t} + u_i \frac{\partial \theta}{\partial x_i} = K_h \left(\frac{\partial^2 \theta}{\partial x_i^2} \right) + Q_h \quad (4)$$

$$\frac{\partial q}{\partial t} + u_i \frac{\partial q}{\partial x_i} = K_q \left(\frac{\partial^2 q}{\partial x_i^2} \right) + Q_q \quad (5)$$

Similar to the momentum equations, Q_h and Q_q are used to link heat and vapor exchange at the plant surface with the atmospheric model. The quantity of Q_h and Q_q is provided by the vegetation model described later on.

2.3 Turbulence and Exchange Processes

Turbulence is produced as flow is sheared near building walls and vegetation. Under windy conditions, the magnitude of local turbulence production normally surpasses its dissipation, so that turbulent eddies are transported by the mean flow. This leads, depending on the structure of the flow, to an increased turbulent exchange away form the original source. To simulate these processes an 2.5order turbulence closure model is needed. Based on the work of Mellor and Yamada [1975] two additional equations for the local turbulence (E) and its dissipation rate (ε) are added to the model:

$$\frac{\partial E}{\partial t} + u_i \frac{\partial E}{\partial x_i} = K_E \left(\frac{\partial^2 E}{\partial x_i^2} \right) + Pr - Th + Q_E - \varepsilon$$

$$\frac{\partial \varepsilon}{\partial t} + u_i \frac{\partial \varepsilon}{\partial x_i} = K_\varepsilon \left(\frac{\partial^2 \varepsilon}{\partial x_i^2} \right) + c_1 \frac{\varepsilon}{E} Pr - c_3 \frac{\varepsilon}{E} Th - c_2 \frac{\varepsilon^2}{E} + Q_\varepsilon \quad (6,7)$$

The terms Pr and Th describe the production and dissipation of turbulent energy due to wind shearing and thermal stratification, Q_ε and Q_ε are the local source terms for turbulence production and dissipation at vegetation. The mechanical production Pr is parameterized using the three-dimensional deformation tensor of the local wind field:

$$Pr = 2K_m \left(\frac{\partial u}{\partial x} \right)^2 + K_m \left(\frac{\partial u}{\partial y} + \frac{\partial v}{\partial x} \right)^2 + K_m \left(\frac{\partial u}{\partial z} + \frac{\partial w}{\partial x} \right)^2 + 2K_m \left(\frac{\partial v}{\partial y} \right)^2 + K_m \left(\frac{\partial v}{\partial z} + \frac{\partial w}{\partial y} \right)^2 + 2K_m \left(\frac{\partial w}{\partial z} \right)^2 \quad (8)$$

The buoyancy production is given by

$$Th = \frac{g}{\theta_{ref}(z)} K_h \frac{\partial \theta}{\partial z} \quad (9)$$

and normally neglected under stable conditions (Th > 0).
To calibrate the ε-equation standard values c_1=1.44 c_2=1.92 and c_3=1.44 given by Launder and Spalding [1974] have been used. Depending on the flow problem, one might use different values for special conditions.
Following Liu et al. [1996] and Wilson [1988] two extra source terms are added to the E-ε System to consider the additional turbulence produced at vegetation as well as the accelerated cascade of turbulence energy from large to small scales near to plant foliage elements:

$$Q_E = c_{d,f} LAD(z) \cdot W^3 - 4c_{d,f} LAD(z) \cdot |W| \cdot E \quad (10)$$

$$Q_\varepsilon = 1.5c_{d,f} LAD(z) \cdot W^3 - 6c_{d,f} LAD(z) \cdot |W| \cdot \varepsilon \quad (11)$$

The latter one is found by the Kolmogorov relation (Launder and Spalding, 1974) and should be adjusted by measured data if available (Liu et al., 1996).

From the calculated E-ε field the turbulent exchange coefficients are calculated assuming local turbulence isotrophy using the relationship

$$K_m = K_h = K_q = c_\mu \frac{E^2}{\varepsilon}; \; K_E = \frac{K_m}{\sigma_E}; K_\varepsilon = \frac{K_m}{\sigma_\varepsilon} \quad (12)$$

with $c\mu$=0.09, σ_E=1 and σ_ε=1.3. To simulate boundary layer flows under different thermal stratification, additional scaling functions given by Sievers et al. [1987] and Businger et al. [1971] are needed to adjust the exchange coefficients.

2.4 Radiative Fluxes

The incoming shortwave and longwave fluxes at the model top can are calculated by a two-stream approximation and some empirical formula (Taesler and Anderson 1984, Gross 1991).
The variation of radiation inside the model due to absorption by plants or shading by buildings are taken into account using reduction coefficients σ_{sw} and σ_{lw} ranging from 1 for undisturbed flux to 0 for total absorption. They are calculated for each grid point by analyzing the model using a ray-tracing algorithm (Bruse 1995).

3. THE SOIL MODEL

As soil types inside urban environments vary over a wide range including surfaces covered by concrete or asphalt, individual thermodynamic and hydraulic properties can be selected for each grid cell in order to simulate different soils profiles and patches of surfaces.
Neglecting horizontal transfers, the soil is treated as a vertical column in which the distribution of heat T and soil volumetric moisture content η are given by:

$$\frac{\partial T}{\partial t} = \kappa_s \frac{\partial^2 T}{\partial z^2} \quad (15)$$

$$\frac{\partial \eta}{\partial t} = D_\eta \frac{\partial^2 \eta}{\partial z^2} + \frac{\partial K_\eta}{\partial z} - S_\eta(z) \quad (16)$$

For natural soils thermal diffusivity κ_s is a function of soil moisture η and can be calculated after Tjernström [1989]. The hydraulic parameters used in (16) are: volumetric water content η, its saturation value η_s, the hydraulic conductivity K_η and the hydraulic diffusivity D_η. All coefficients are calculated using the formulae given by Clapp and Hornberger [1978]. The water uptake by the plant roots S_η is provided by the vegetation model and treated as an internal sink of moisture.

4. THE VEGETATION MODEL

Vegetation is treated as a one-dimensional column with height z_p with a given leaf area density (LAD) profile. Inside the soil system the distribution of roots is represented by the root area density (RAD) profile with total depth $-z_r$. This scheme is universal and can be used for small plants like grass or crop as well as for huge trees.
The interactions between the plant leafs and the surrounding air can be expressed in terms of direct heat flux $J_{f,h}$, evaporation flux $J_{f,evap}$ and transpiration flux $J_{f,trans}$:

$$\begin{aligned} J_{f,h} &= 1.1 r_a^{-1}(T_f - T_a) \\ J_{f,evap} &= r_a^{-1}\Delta q \delta_c f_w \\ J_{f,trans} &= \delta_c (r_a + r_s)^{-1}(1 - f_w)\Delta q \end{aligned} \qquad (17a,b,c)$$

T_a and q_a are the temperature and the specific humidity of the air. Δq is the humidity difference with $\Delta q = q_*(T_a)-q_a$. T_f is the foliage temperature and q_* the saturation value of q at the leaf surface. Following Barden [1982], the aerodynamic resistance r_a is a function of the leaf geometry and wind speed:

$$r_a = A(D/W)^{0.5} \qquad (18)$$

where W= wind speed at the leaf surface $A=87\ sec^{0.5}m^{-1}$ for conifers and grass and $A=200\ sec^{0.5}m^{-1}$ for deciduous trees. D is the typical leaf diameter ranging from 0.02 m for conifers up to 0.5 m or more for tropical plants (Schilling, 1990). The stomatal resistance r_s is calculated with respect to radiation input and water content inside the root zone as described by Deardorff [1978].
The factor δ_c is set to 1 if evaporation and transpiration are possible ($\Delta q \geq 0$), otherwise δ_c is 0 and only condensation is possible. Assuming that only wet part of the vegetation can evaporate (17b) and, on the other side, only dry parts will transpire (17c), the fraction of wet leaves inside one grid box is needed. Following Deardorff [1978] the fraction of wet foliage is given by

$$f_w = (W_{dew} / W_{dew,max})^{2/3} \qquad (20)$$

where W_{dew} is the actual amount of dew on the leave surfaces and $W_{dew,max}$ is the maximum possible value ($0.2\ kgm^{-2}$)
After each time step the distribution of dew inside one grid box in a vertical pant column is recalculated and dew exceeding the maximum value will be transported to the box below or will be added to the soil water balance in case of the last grid box with vegetation above the surface.

Neglecting internal energy storage inside a thin leaf, the foliage temperature T_f can be obtained from the leaf energy budget:

$$0 = R_{sw,net} + R_{lw,net} - c_p\rho J_{f,h} - \rho L(J_{f,evap} + J_{f,tran}) \qquad (21)$$

where c_p is the specific heat of the air and ρ the air density, L is the latent heat of vaporization.
$R_{sw,net}$ and $R_{lw,net}$ are the net shortwave and longwave radiation absorbed by the leave surface.
The source/sink terms for the atmospheric model can be computed after solving (21) with:

$$Q_h(z) = LAD(z)J_{f,h} \qquad (22)$$

$$Q_q(z) = LAD(z)(J_{f,evapo} + J_{f,trans}) \qquad (23)$$

where LAD is the leaf area density in height z. Inside the soil model, water loss due to root uptake must balance the plants total transpiration m_{trans} :

$$m_{trans} = \rho \int_0^{z_p} LAD(z)J_{f,trans}(z)dz \qquad (24)$$

where z_p is the total plant height. After Pielke [1984] the water loss in soil layer -z is

$$S_\eta(-z) = \frac{m_{trans}}{\rho_w}(RAD(-z)D_\eta(-z))\left(\int_{-z_r}^{0} RAD(-z)D_\eta(-z)dz\right)^{-1} \qquad (25)$$

RAD is the root area density in depth -z and z_r is the depth of the root zone.

5. GROUND SURFACE AND WALLS

The turbulent fluxes of momentum, heat and vapor at the ground surface and at walls are calculated using the similarity law from Monin and Obhukov:

$$J_m^0 = u_*^2 \ ; \ J_h^0 = u_*\theta_* \ ; \ J_q^0 = u_*q_* \qquad (26\ a,b,c)$$

The scaling velocities of momentum (friction velocity) u_*, heat θ_* and vapor q_* are calculated with respect to thermal stratification (Asaeda et al. 1993). In case of free convection the *Convective Transport Theory* (Stull 1994) is used to describe vertical transport by thermals.
Temperature T_0 at the ground surface can be calculated from the energy balance

$$0 = R_{sw,net} + R_{lw,net} - \sigma_f c_p \rho J_h^0 - \sigma_f \rho L \cdot J_q^0 - G \qquad (27)$$

$R_{sw,net}$ and $R_{lw,net}$ are the net shortwave and longwave radiation absorbed by the surface calculated with respect to the temperatures of surfaces and walls „seen" by the ground.
The shielding factor σ_f is only used for small plants directly covering the ground and prevent sensible and latent fluxes in the covered fraction. Surface humidity q_0 can be calculated from the soil moisture content al level z=-1 using the β-approach from Deardorff [1978]:

$$\begin{aligned} q_0 &= \beta q_*(T_0) + (1-\beta)q(z=1) \\ \beta &= \min(1, \eta(z=-1)/\eta_{fc}) \end{aligned} \qquad (28)$$

where η_{fc} is the field capacity of the soil at level -1.

6. NUMERICAL ASPECTS

6.1 Solution Techniques

All differential equations are approximated using the finite difference method and solved forward-in-time.
To solve the combined advection-diffusion equations, the Alternating Directions Implicit Method (ADI) in combination with an upstream advection scheme is used.
Dynamic pressure is removed from the equations of motion (xx) and calculated separately from the Poisson equation

$$\nabla^2 p' = \frac{\rho}{\Delta t} \nabla \mathbf{u}^{aux} \tag{29}$$

using the Simultaneous Over Relaxation (SOR) method with $\mathbf{u}^{aux}$ as the auxiliary flow calculated without any pressure correction and Δt = time step (Patrinos and Kistler, 1977).

6.2 Computational Domain and Grid Structure

Depending on the problem, the total size of the three dimensional model X,Y and Z as well as the resolution of the grid can be selected within a wide range. Equidistant spacing Δx, Δy and Δz is used in each direction (only the lowest grid cell above ground is split into 5 cells with size $\Delta z_g = 0.2\Delta z$ to increase accuracy in calculating surface processes). The three dimensional model is nested into a one dimensional model which extends up to 2500 m height. The values of the one dimensional model are used as reference values as well as inflow profiles and top boundary conditions for the three-dimensional model.

7. MODEL RESULTS

To show the basic characteristics of the model we restrict ourselves to two simple examples simulating the exchange processes at and in a block of buildings (height 20 m) with two entrance gates (5 m). The basic soil used in both cases is an 6 cm thick asphalt surface above a 2 cm layer of sand followed by loam down to a depth of 2 m. The good insulation of sand and the small asphalt layer will lead to quite high temperatures when the sun shines onto the surface. The first example (EX 1) only consists of these asphalt surfaces. In the second example (EX 2), the surface inside the block was replaced by loam covered with grass and a block of trees (20 m height). Another row of trees is placed on the windward side of the block All presented results are shown for 12.00 h local time, the other basic input parameters are summarized in Table 1.
Figure 1 shows the horizontal flow in and around the block without any vegetation at z= 2 m. As both entrance gates lies on opposite sides, the wind can blow through the block at this height. Jet effects can be observed at the gates and small horizontal eddies are found in the lee of the block and between the buildings.

Table 1: Basic input parameters for both studies

Location	42.90° s. Lat., 147.30° e. Long. (Hobart)
Date, Time	23.12, 12..00
Initial Wind	3 m/s at 10 m from 90° (East)
Boundary Conditions	θ (2500 m)= 290 K, q (2500 m)= 0.002 g/g
Grid Size	35 x 25 x 25 Grids, $\Delta x=\Delta y=\Delta z$= 2 m
Plants	**Dense Tree:** z_p= 20 m r_s= 400 sm^{-1} Normalized LAD Profile (z/z_p=0.1, 0.2.. 1.0) 0.15, 0.15, 0.15, 0.15, 0.65, 2.15, 2.18, 2.05, 1.72 **Gras:** z_p= 0.50 m r_s= 200 sm^{-1} Overall LAD: 2.00
Walls	T=290 K (kept constant), q=0
Soil	T (-2m)= 290K; Initial Wetness: 50 % Saturated

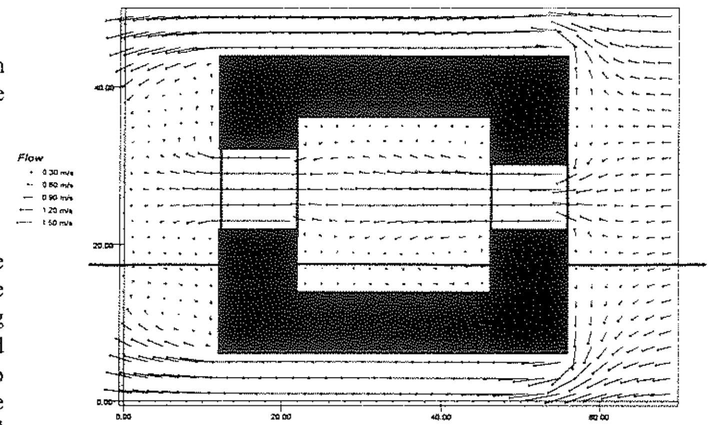

Figure 1: Horizontal flow for EX1 at z=2m

The distribution of temperature at z=2 m is shown in Figure 2, the arrow marks the position of the sun. All values are normalized with the temperature at the inflow boundary at the same level. In this case this reference profile is defined as a well-mixed layer over an unshaded asphalt road

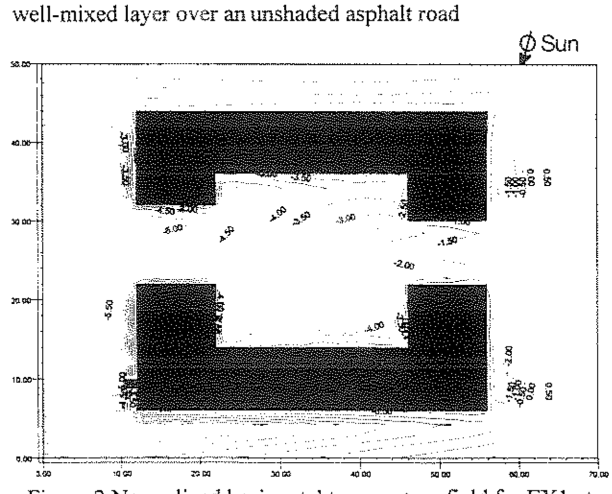

Figure 2:Normalized horizontal temperature field for EX1 at z=2m, Contour Interval 0.5 K

As the buildings are close to each other, most of the yard remains shaded and the surface temperature is much lower than in the sunlit parts. The air blown through the gate on the left side starts to cool down as it passes the yard. The observed lower temperatures *before* entering the yard are due to downward motion of colder air from higher levels as an effect of the gate.

Horizontal results for EX2 are not shown as the focus for further analyses will be set on vertical cuts. Figure 3 shows the vertical flow at y= 19 m (see line in Figure 1) for the case without vegetation (top) and with vegetation (bottom). The light gray bars indicate vegetation with a LAD ranging from 0.1 to 1.5, the dark gray bars stand for a LAD above 1.5.

Typical elements of flow dynamics near to solid obstacles can be found in Figure 3. Upwind from the right wall a downward flux area can be observed in EX1 with a stagnation point at ½ of the building height whereas in the upper half the flow is directed upward. In case of EX2, the downward flux area is much smaller whereas the area of upward directed wind has increased. This is caused by flow canalization inside the trees which prevents the vortex eddy from further vertical and horizontal extension

Inside the yard a typical circulation system has established with an upward directed flux along the right building facade and a downward flux on the opposite side. Due to jet effects between the building walls and the vegetation a higher vertical wind speed can be observed along the wall in the EX2. The wind speed inside the dense parts of the crown layer is reduced and the symmetry of the circulation is modified. As the average wind speed inside the yard is below 0.50, modification by drag forces at vegetation become low.

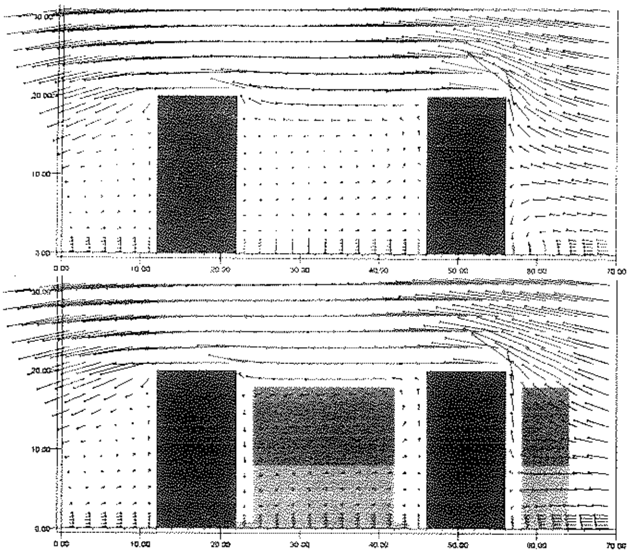

Figure 3:Vertical flow profiles in the lower part of the model

More differences between EX1 and 2 can be found in comparing the vertical plot of normalized temperature in Figure 4. In EX1 the upward directed flow on the upstream side of the block advects warmer air from near-surface layers up to the roof top area where it is transported over the yard and mixed by downward advection with colder air inside the yard. Although the surface is shaded this transport leads to higher temperatures in the upper half of the in-yard air. In the lower half the cooler yard ground leads to relative cold air. This effects together cause a strong stable stratification inside the yard.

In case of EX2 the distribution of temperature differs much more than the modifications of the flow: The direct radiation causes a local temperature maximum of +2.00 K in the crown layer of the upwind trees. In contrast, the trees inside the yard are shaded and much colder than the surrounding air. Due to this air transported over the right building is warmer than in case 1 but it is cooled down as it passes the leaves of the trees in the yard.

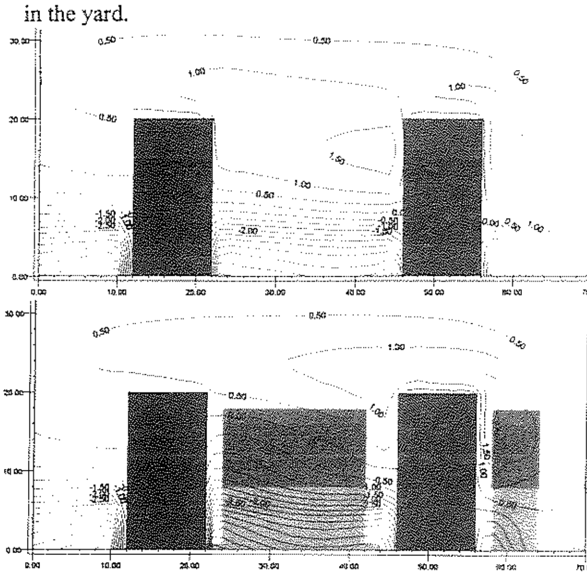

Figure 4: Vertical plot of normalized temperatur, Contour Intervall 0.5 K

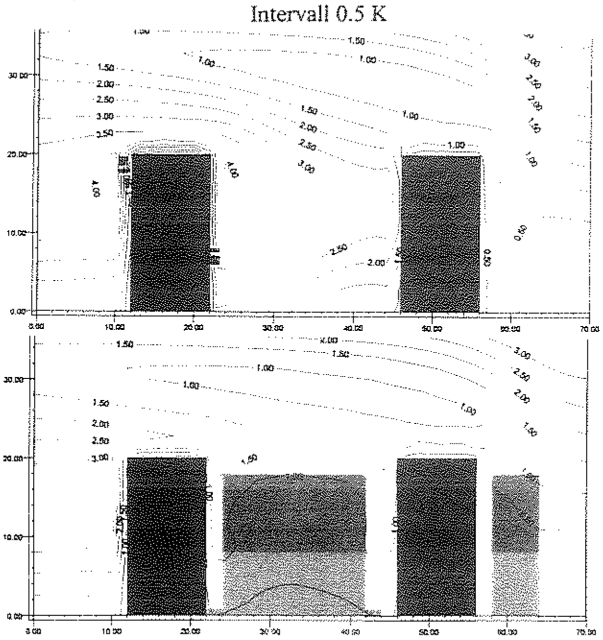

Figure 5: Vertical plot of turbulent exchange coefficient, Contour Intervall 0.5

The profile of the turbulent exchange coefficient Km as a function of the E-ε distribution is shown in Figure 5. In the vegetated case turbulence and vertical mixing in the yard and with the air above roof level is reduced whereas in EX1 the in-yard air is well mixed with a local maximum at the upper parts of the left building.

The trees in front of the upwind building cause a nearly constant exchange coefficient up to 15 m height whereas the turbulence field in case 1 is driven by the vortex eddy in the lower half of the building.

Above 30 m the effects of vegetation become low and the profile of Km shows a vertical displacement of approximately 15 m = ½ building height

8. CONCLUSIONS

Only a small insight in the complex interactions between the surface, plants and the atmosphere could be given here.

It was shown that the processes are highly nonlinear and can not be estimated by some rule of thumb. For example, if the trees inside the yard were absent, and only the trees in front of the buildings would remain, this could lead to an increased air temperature inside the yard.

If one has to make a valuation on how small scale environmental design changes microclimate, it is impossible to assess all changes just by a linear combination of known single facts. There is the need of computer-based tools to estimate the effects of different ideas in order to optimize the climate we live in.

9. REFERENCES

Asaeda et al., The subsurface transport of heat and moisture and its effect on the environment: A numerical model, *Boundary Layer Met.*, 65,159-179, 1993

Barden, H., Simulationsmodell für den Wasser-, Energie- und Stoffhaushalt in Pflanzenbeständen, *Rep. Inst. Met. Univ. Hanover*, 23, 1982

Bruse, M., Development of a microscale model for the calculation of surface temperatures in structured terrain, MSc Thesis, Inst. for Geography, Univ. Bochum, 1995

Businger J. A. et al., Flux profile relationships in the atmospheric surface layer, *J. Atmos. Sci.*, 28, 181 189, 1971

Clapp R. B. and G. Hornberger, Empirical equations for some soil hydraulic properties, *Water Resource. Res.*, 14, 601-604, 1978

Deardorff, J. W., Efficient prediction of ground surface temperature and moisture with inclusion of a layer of vegetation, *J. Geophys. Res.*, 83,1889-1903, 1978

Eichhorn, J., Entwicklung und Anwendung eines dreidimensionalen mikroskaligen Stadtklimamodells, PhD- Thesis, Univ. Mainz, D, 1989

Gross, G., Anwendungsmöglichkeiten mesoskaliger Simulationsmodelle dargestellt am Beispiel Darmstadt, *Meteorol. Rundschau*, 43, 97-112, 1991

Gutman; D. P. and K. E. Torrance, Response of the urban boundary layer to heat addition and surface roughness, *Boundary Layer Met.*, 9, 217 - 233, 1975

Hirt , C. W. and J. L. Cook, Calculating three-dimensional flows around structures and over rough terrain, *J. Comput. Phys.*, 10, 324 -340, 1972

Launder B.E. and D. B. Spalding, The numerical computation of turbulent flows, *Comp. Methods Appl. Mech. Eng.*, 3, 269-289, 1974

Liu J. et al. E-ε modelling of turbulent air flow downwind of a model forest edge, *Boundary Layer Met.*, 77, 21-44, 1996

Mellor G. L. and T. Yamada, A simulation of the Wangara atmospheric boundary layer data, *J. Atmos. Sci.* 32, 2309-2329, 1975

Patrinos A. A. and A. L. Kistler, A numerical study of the chicago lake breeze, *Boundary Layer Met.*, 93.123, 1976

Pielke R. A., *Mesoscale meteorological modelling*, Academic Press, Orlando, 1984

Schilling, V., A parameterization for modelling the meteorological effects of tall forests - A case study of a large clearing, *Boundary Layer Met.*, 55, 283-304, 1991

Sievers, U. et al., Numerische Simulation des urbanen Klimas mit einem zweidimensionalen Modell, *Meteorol. Rundschau* 40(1/3), 40 - 52 /65-83, 1987

Stull, R., A convective transport theory for surface fluxes, *J. Atmos. Sci.*, 51, 3-22, 1994

Taesler R. and C. Anderson, A method for solar radiation computings using routine meteorological observations, *Energy and Buildings*, 7, 341-352, 1984

Terjung W. H. and P. O' Rourke, Simulating the causal elements of urban heat islands, *Boundary Layer Met.* 19, 93 -188, 1980

Tjernström, M., Some tests with a surface energy balance scheme including a bulk parameterization for vegetation in a mesoscale model, *Boundary Layer Met.*, 48, 33-68, 1989

Wang H. and E. S. Takle, A numerical simulation of boundary layer flows near shelterbelts, *Boundary Layer Met.*, 48, 33 68

Watanabe, T., Bulk parameterization for a vegetated surface and its application to a simulation of nocturnal drainage flow, *Boundary Layer Met.*, 70, 13 -35, 1994

Wilson, J. D., A second order closure model for flow through vegetation, *Boundary Layer Met.* 42, 371-392, 1988

Yamada , T., A numerical model study of turbulent airflow in and above a forest canopy, *J. Met. Soc. Japan*, 60, 439-454, 1982

Authors address:
Michael Bruse,
Research Group Climatology, Department of Geography,
Ruhr-University Bochum,
Universitaetsstrasse 150,
D-44780 Bochum, Germany,
(+49) 234- 700- 4244
e-mail: michael.bruse@ruhr-uni-bochum.de